Dependence of MaxWISE Position, Proper Motion, and Parallax Estimation Uncertainties on Attenuation Strategy

Document number: WSDC-D-T044

1. Overview

Compared to AllWISE, MaxWISE will have on average about four times as many samples at any given sky location and about 13 times the chronological baseline for estimating proper motion (e.g., from January 20, 2010 to July 20, 2016, instead of to July 20, 2010, since most AllWISE source motions are estimated from a six-month baseline). Scaling from the AllWISE sky coverage pattern (http://wise2.ipac.caltech.edu/docs/release/allwise/expsup/sec4_2.html) suggests that a density of 250 or more coverages will exist at ecliptic latitudes within about 25 degrees of a pole. This will require "attenuation", since hardware limitations will restrict the number of measurements that can be used in the WPHotpm program to about 250. We use a maximum of 248 because that is divisible by the number of MaxWISE "epochs", 8, with no remainder. The number of coverages at several ecliptic latitudes as assumed herein are:

Beta	AllWISE Cov	MaxWISE (4x AllWISE up to 248)	MaxWISE/epoch
0	24	96	12
30	30	120	15
45	36	144	18
60	54	216	27
75	80	248	31
80	100	248	31
85	128	248	31
90	128	248	31

The choice of which measurements to retain at high latitudes affects the formal uncertainties of estimated parameters, in this case proper motion and parallax in addition to position. Proper motion benefits from concentrating measurements at the extreme ends of the chronological span; parallax benefits from keeping all measurements in pairs separated by six months. A quantitative measure of these effects is desired in order to guide attenuation strategy, as well as to get some feeling for how much MaxWISE will improve upon AllWISE.

To achieve this, a simulation of the 84-month MaxWISE period has been implemented. Simulated observations of a source at specified ecliptic coordinates are generated for various sets of measurement times. These are processed by a chi-square minimization algorithm based on a model that includes position, proper motion, and parallax. This algorithm differs from the WPHotpm algorithm in that the latter estimates flux at the same time as position, proper motion, and parallax; it does this by searching numerically for a chi-square minimum in the parameter space, where chi-square is defined in terms of flux discrepancies relative to flux uncertainties. The simulation takes the positions as being the fundamental measurements, and chi-square is defined in terms of position

uncertainties. Because both algorithms are optimal, the flow of common uncertainties should be parallel, so that the final parameter uncertainties in the simulation should behave the same as the corresponding ones in the WPHotpm algorithm. Analysis of the WPHotpm error covariance matrix has shown that the position and motion uncertainties do indeed behave in the same way as those of the simulation. For example, the dependence of the correlation between position error and motion error on the choice of the time zero point is exactly the same in both algorithms.

The other main difference between this simulation and the WPHotpm algorithm is that the latter operates in celestial coordinates, whereas simulating parallax is much more straightforward in ecliptic coordinates, and so the simulation uses ecliptic coordinates throughout. The information content is identical, and so this has no effect on estimation accuracy. Because of the WISE observing geometry, ecliptic latitude measurements contribute negligibly to the parallax estimation except very close to the ecliptic poles. The WPHotpm algorithm will obtain parallax information from both RA and Dec positions, but again the information content is identical in the two formulations. RA and Dec generally both contribute to the estimation of a single parallax parameter; the parallax is not treated as having components on two axes, it is a scalar that contributes observational offsets to both axes which are combined in the WPHotpm algorithm to produce a single number. In the simulation, this is accomplished by inverse-variance averaging of the estimates obtained from longitude and latitude. This is done only to show that including a latitude contribution does not degrade the final estimate; the parallax sampling in latitude is so poor that it always produces an uncertainty vastly larger than that of the longitude contribution, and the final estimate is essentially equal to the longitude estimate.

The unit of time employed is the "month", essentially a 30.4375-day period of time zeroed at Jan 20, 2010. The simplified epoch definitions are:

m = 0 on Jan 20, 2010 (approximate start of AllWISE)
m = 12 on Jan 20, 2011 (approximate end of AllWISE)
m = 12 to 48 empty (no measurements taken)
m = 48 to 84 is the MaxWISE period

A given point on the sky is considered observable once per orbit if its ecliptic longitude is close to 90 degrees different from the Earth's as seen from the sun. The Earth's orbit is approximated as circular with ecliptic longitude given by 30*(m-2)+180 degrees, i.e., at m = 2 (March 20, 2010), Earth is at 180 degrees longitude (i.e., the sun as seen from the Earth is at 0 degrees longitude).

There should be no significant dependence of measurement error on source ecliptic longitude, and so for convenience, the simulations consist of setting the star's position at a longitude of 90 degrees and various latitudes; this star can then be observed during times close to the equinoxes, and various sets of measurement times can be selected to explore attenuation strategies. Within 65 degrees of the ecliptic, all measurements can be used, and so the option of clustering measurement times at the mission extremes is irrelevant, and all measurement times are automatically paired with 6-month offset times. The value of these cases is strictly in estimating the uncertainties of the proper motion and parallax determinations. Above 65 degrees, some measurements must be discarded, and above 85 degrees, it is geometrically possible to depart from the 6-month-separation-time pairing.

2. Simulation of a Given Measurement

Since the uncertainty σ_μ of the proper motion μ estimated from a sample of measurements via chi-square minimization is independent of the proper motion itself (as shown in section 3 below), we can choose any value for the simulation, and the same is true of the parallax p. The point of choosing specific values is that this allows us to verify that the simulation is working correctly, since we ought to recover the "true" values within a small number of standard deviations representing the uncertainty of the estimates. All stars simulated were assigned proper motion on both axes of 1 arcsec/yr and parallax of 1 arcsec.

The parallax parameter, which we denote p herein, is new to the WISE data processing. It is a single parameter for a given source, but in general it affects position on both axes through projection coefficients. In ecliptic coordinates, and given the WISE observing constraints, the latitude projection coefficient is generally very small, as will be seen below, and this results in very little parallax information getting into the latitude position data.

Since parallax is induced by the orbital motion of the Earth, by symmetry its pattern is easily envisioned as the trajectory of the Earth about the sun as seen from the star, but with a phase difference of 180 degrees. Since a star near the ecliptic sees the Earth's orbit as essentially oscillating along a straight line, there is very little latitude variation. At higher ecliptic latitudes, the elliptical shape of the projection of the Earth's orbit is more apparent, but because measurements are taken only when the Earth is very close to the extreme longitude excursions, very little latitude information is captured. The information available for estimating the star's parallax is the same as though the Earth's orbital trajectory were being estimated from the star, but using only measurements taken when the Earth is very near its extreme longitude excursions. So even if the star is at a high ecliptic latitude, it never sees the Earth with any significant latitude excursion. The same is true of the star as seen from the WISE spacecraft.

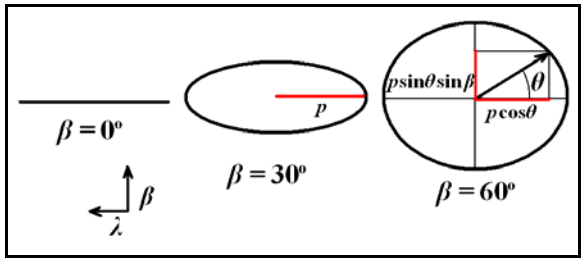

The schematic on the left shows the Earth's orbit as seen from three stars with parallax p and ecliptic latitudes of 0°, 30°, and 60°. Approximated as a circle, the Earth's orbit appears as an ellipse with semimajor axis p and semiminor axis $p\sin\beta$. When the Earth is at a position corresponding to an angle θ *in its circular orbit*, the star sees the full longitude component $p\cos\theta$ and the foreshortened latitude component $p\sin\theta\sin\beta$. The angle θ is zero when the Earth's ecliptic longitude relative to the sun is 90° greater than the star's ecliptic longitude, so $\theta = (\lambda_E - \lambda) - 90^\circ$. We denote the angle corresponding to θ when viewing the star from Earth as φ; then $\varphi = \theta + 180^\circ = (\lambda_E - \lambda) + 90^\circ$; then $\cos\varphi = -\sin(\lambda_E - \lambda) = \sin(\lambda - \lambda_E)$, and $\sin\varphi = \cos(\lambda_E - \lambda) = \cos(\lambda - \lambda_E)$.

The i^{th} position measurement (λ_i,β_i) of a star with true ecliptic coordinates (λ_0,β_0) at $m = 0$, true proper motion (μ_λ,μ_β), true parallax p, measurement errors $(\varepsilon_{\lambda i},\varepsilon_{\beta i})$, and a time tag m_i is simulated as

$$\begin{aligned} \lambda_i &= \lambda_0 + \left(\mu_\lambda m_i + p\sin(\lambda_0 - \lambda_{Ei}) + \varepsilon_{\lambda_i}\right)/\cos\beta_0 \\ \beta_i &= \beta_0 + \mu_\beta m_i + p\cos(\lambda_0 - \lambda_{Ei})\sin\beta_0 + \varepsilon_{\beta_i} \end{aligned} \qquad (1)$$

where λ_{Ei} is the ecliptic longitude of the Earth at the time m_i, and the proper motions and parallax are in true angular measure. Technically, the arguments of the sine and cosine functions should be $(\lambda_i - \lambda_{Ei})$, and β_i, but this would require iterating the equations, and the position errors induced by the approximation error of a few arcseconds in the trigonometric arguments are negligible compared to the simulated errors. The measurement uncertainties and errors in arcsec were simulated as

$$\begin{aligned} \sigma_{\lambda i} &= 0.4 + 0.15U(0,1) \\ \sigma_{\beta i} &= 0.4 + 0.15U(0,1) \\ \varepsilon_{\lambda i} &= \sigma_{\lambda i}\ G(0,1) \\ \varepsilon_{\beta i} &= \sigma_{\beta i}\ G(0,1) \end{aligned} \tag{2}$$

where each $U(0,1)$ is an independent draw from a uniform distribution on the interval (0,1), and each $G(0,1)$ is an independent draw from a zero-mean unit-variance Gaussian distribution. These uncertainties and errors are quite conservative; the sigmas vary uniformly between 0.4 and 0.55 arcsec. For comparison, typical position uncertainties for sources used in distortion calibration are about 0.130 to 0.145 arcsec.

The measurement times used in the chi-square minimization for the baseline strategy, i.e., the same number of measurements from each "epoch" (i.e., passage of a source through the WISE observing region near 90 degrees elongation) was as follows, where `MperEpoch` is taken from the last column in the table in section 1 for the latitude being simulated.

```
i = 0
For Nepoch = 1 to 8 do
      For n = 1 to MperEpoch
            i ⇒ i+1
            m_i = (Nepoch-1)*6 + 2 + 0.002083*(n-MperEpoch/2)
            if (Nepoch > 2) then m_i ⇒  m_i+36
      End {For n}
End {For i}
```

where 0.002083 is the orbital period in months. The distribution of observed ecliptic longitude over time for a source at 30 degrees latitude with a parallax of 1 arcsec and per-axis proper motions of 1 arcsec/year can be seen in the plot on the right.

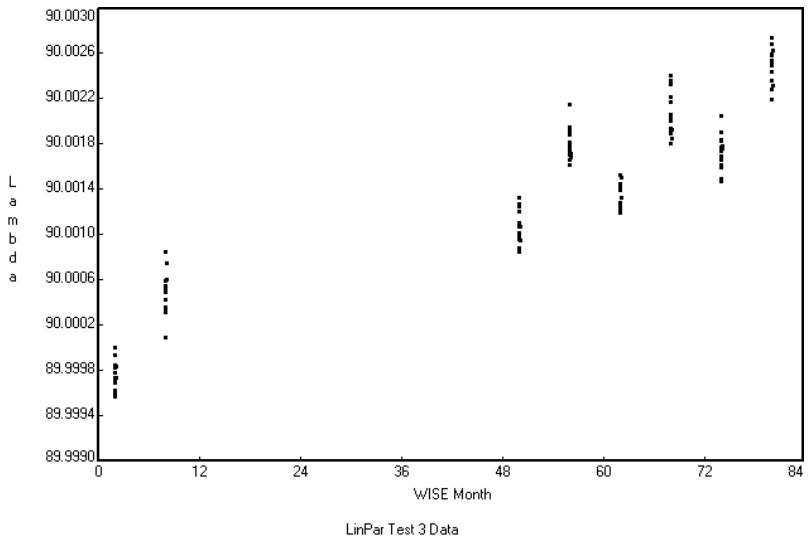

Above ecliptic latitude 65°, not all measurements can be used because of computing limitations, so there is some freedom to choose less uniform sampling in the time domain. This has no effect on the position

estimation accuracy, but clustering observation times near the extremes would improve proper motion accuracy. As long as every measurement has a corresponding measurement at a time six months different, parallax estimation accuracy will be as good as it can be. The other consideration is detecting flux variability, for which the WISE mission has no requirements and was not optimized. Clustering measurement times near the extremes would reduce the sensitivity to variability at the intermediate time scales, e.g. one year, while it would probably improve accuracy on shorter time scales for periodic variability.

3. Chi-Square Minimization Algorithm

The fact that the uncertainty of parameters estimated via chi-square minimization does not depend at all on the actual measured values but only on the sampling and measurement uncertainties can be somewhat non-intuitive, and so we will give a brief review of why this is true. One point to be stressed is that the chi-square goodness-of-fit figure of merit should always be evaluated, because that indicates whether the model is reliable. By "the model", we mean the form of the function to which the measurements are fit, the measurement uncertainties, and the absence of outliers due to unmodeled effects (e.g., cosmic rays).

In general, given N data points y_i with uncertainties σ_i, $i = 1$ to N, and each data point associated with an abscissa x_i, we wish to model y as a function of x with a functional dependence of the form

$$y = \sum_{k=1}^{M} c_k \, f_k(x) \tag{3}$$

where the c_k are coefficients whose values must be found, and the f_k are M arbitrarily chosen *basis functions* that define the model. For example, if we wish to use a cubic polynomial model, then $f_k(x) = x^{k-1}$, and $M = 4$. In order to solve for M model coefficients, we must have $N \geq M$, and for chi-square to be meaningful, we must have $N > M$. In typical cases, $N >> M$.

We have deliberately made the functional dependence linear with respect to the c_k coefficients. The basis functions may be anything at all as long as they can be evaluated at the abscissa values (hence they may not be explicit functions of c_k); they may even be functions of both x and y, since the y_i are also known, but since the y_i are uncertain, any basis function that depends on them will also be uncertain, and in the chi-square minimization below, this will cause the c_k to appear in the denominators, making the system of equations that we have to solve nonlinear. Nonlinear systems can be solved via iterative methods, but the subject is far removed from the present scope and not relevant to the current problem. We also assume that the abscissa values are known exactly, since if they also have uncertainties, that too results in the c_k appearing in the denominators of the equations we have to solve, which would therefore again be nonlinear.

If the uncertainties in the data describe errors that may be approximated as zero-mean Gaussian random variables, then Gaussian estimation may used to evaluate the coefficients c_k, and from this it follows that chi-square minimization is the optimal method to employ. For uncorrelated errors, chi-square is the sum of the ratios of the squared differences between the model and the observed values

divided by the uncertainty variance:

$$\chi^2 = \sum_{i=1}^{N} \frac{\left(y_i - \sum_{k=1}^{M} c_k \, f_k(x_i) \right)^2}{\sigma_i^2} \tag{4}$$

The number of independent terms summed minus the number of parameters used in the fit is called the *number of degrees of freedom* of the χ^2 random variable, D_F, in this case N-M.

In order to solve for the values of c_k that minimize χ^2, we set the derivatives of the latter with respect to the former to zero. This results in M equations in the M unknown coefficients c_k, forming a linear system that can be solved by standard methods. Each equation has the form

$$\begin{aligned} \sum_{i=1}^{N} \frac{y_i \, f_k(x_i)}{\sigma_i^2} &= \sum_{i=1}^{N} \frac{f_k(x_i) \sum_{j=1}^{M} c_j \, f_j(x_i)}{\sigma_i^2} \\ &= \sum_{j=1}^{M} c_j \sum_{i=1}^{N} \frac{f_k(x_i) \, f_j(x_i)}{\sigma_i^2} \end{aligned} \tag{5}$$

where we have interchanged the summation order of the right-hand side on the second line. With the definitions

$$\begin{aligned} b_k &\equiv \sum_{i=1}^{N} \frac{y_i \, f_k(x_i)}{\sigma_i^2} \\ a_{jk} &\equiv \sum_{i=1}^{N} \frac{f_j(x_i) \, f_k(x_i)}{\sigma_i^2} \end{aligned} \tag{6}$$

we obtain an equation which can be written in vector-matrix form as

$$\vec{b} = A \vec{c} \tag{7}$$

where the matrix A has elements a_{jk} and is called the *coefficient matrix*, because it contains the coefficients of the equations forming the $M \times M$ system of equations. Note that $a_{jk} = a_{kj}$, i.e., A is a symmetric matrix. Note further that A is completely independent of the y_i values; since the error covariance matrix for the c_k solutions is the inverse of A (the derivation will omitted for the sake of brevity), it follows that those uncertainties do not depend on y_i either. Equation 7 can be solved by various techniques, one of which is to employ the inverse of the A matrix: multiplying both sides from the left by A^{-1}, and dropping the identity matrix that results from $A^{-1}A$, yields the equation

$$\vec{c} = A^{-1} \vec{b} \tag{8}$$

If solutions for the c_k are all that is desired, then this is not the most computationally efficient way to proceed, but in fact, because as just mentioned, it is the error covariance matrix for the c_k solutions, we will need the inverse matrix anyway, and so we might as well compute it first and use it to obtain the solution. Fitting errors are typically significantly correlated, so when the model is used to compute a value of y for some chosen value of x, the uncertainty in that value of y should be computed using the full error covariance matrix:

$$\Omega = A^{-1} \equiv \begin{pmatrix} v_{11} & v_{12} & \cdots & v_{1M} \\ v_{21} & v_{22} & \cdots & v_{2M} \\ \vdots & \vdots & \ddots & \vdots \\ v_{M1} & v_{M2} & \cdots & v_{MM} \end{pmatrix} \tag{9}$$

The diagonal elements v_{kk} are the uncertainty variances of the c_k solutions, also commonly denoted $\sigma^2(c_k) = \langle \varepsilon_{ck}^2 \rangle$, where ε_{ck} is the error in c_k. These elements are always positive in practical applications, i.e., uncertainties are always real and greater than zero in real life. Because A is symmetric, its inverse Ω is also. The off-diagonal elements are the error covariances for the model coefficients, i.e., expectation values for the product of the ε_{ck} and ε_{cj}, $k \neq j$, and may be positive, negative, or zero.

Because the model is linear in the c_k coefficients, when the solution is used to compute a y value for some x value, the estimation error ε_y depends on the coefficient errors ε_{ck} in the same way that y depends on the c_k:

$$\varepsilon_y = \sum_{k=1}^{M} \varepsilon_{ck} \, f_k(x) \tag{10}$$

The uncertainty variance for y is the expectation value of the square of ε_y:

$$\begin{aligned} \sigma_y^2 = \langle \varepsilon_y^2 \rangle &= \left\langle \left(\sum_{k=1}^{M} \varepsilon_{ck} \, f_k(x) \right)^2 \right\rangle \\ &= \sum_{k=1}^{M} \langle \varepsilon_{ck}^2 \rangle f_k^2(x) + 2 \sum_{k=1}^{M-1} \sum_{j=k+1}^{M} \langle \varepsilon_{cj} \, \varepsilon_{ck} \rangle f_j(x) \, f_k(x) \\ &= \sum_{k=1}^{M} \sigma^2(c_k) \, f_k^2(x) + 2 \sum_{k=1}^{M-1} \sum_{j=k+1}^{M} v_{jk} \, f_j(x) \, f_k(x) \end{aligned} \tag{11}$$

Once the c_k are known, Equation 4 should be evaluated to verify that the value of χ^2 is reasonable, i.e., close to D_F. "Close" generally means within several standard deviations, where the value of the standard deviation is $\sqrt{(2D_F)}$. If this is not true, then the model is not trustworthy.

For the simulation, Equation 3 takes the form

$$y = c_1 + c_2 x + c_3 g(x)$$

$$\text{for y} \Rightarrow \lambda\text{: } x \Rightarrow m\,,\ c_1 \Rightarrow \lambda_0\,,\ c_2 \Rightarrow \mu'_\lambda\,,\ c_3 \Rightarrow p'\,,\ g(m) \Rightarrow \sin\left(\lambda - \lambda_E(m)\right) \qquad (12)$$

$$\text{for } y \Rightarrow \beta\text{: } x \Rightarrow m\,,\ c_1 \Rightarrow \beta_0\,,\ c_2 \Rightarrow \mu_\beta\,,\ c_3 \Rightarrow p\,,\ g(m) \Rightarrow \cos\left(\lambda - \lambda_E(m)\right)\sin\beta$$

where the primes on μ_λ and p on the line for λ indicate that these apply to the azimuthal angle, not true angular measure, and so after they are obtained they must both be multiplied by cosβ to obtain the corresponding values in local true angular measure.

One final adjustment was made to the algorithm: the zero point for the independent variable m is arbitrary but generally has a strong effect on the fitting error of the intercept and its correlation with the slope error for a straight-line model fit. Often the zero point is left at zero, and with positive abscissa values, the error in the slope and intercept are generally negatively correlated. Significant correlation in the errors must be taken into account when the uncertainty of a model evaluation is computed, i.e., Equation 11. This correlation arises because the straight line generally goes through the middle of any cloud of data points, i.e., with non-pathological measurement errors, the solution will never pass well above or below the middle of the scatter, assuming a linear model is appropriate in the first place. If the zero point is left outside of where most of the points lie, the magnitude of the error in the intercept is generally increased, but the error correlation completely mitigates this when the model uncertainty is evaluated using the full error covariance matrix. Still it is often preferable to translate the independent variable to a different zero point nearer to the middle of the abscissa range, since this reduces the nominal intercept uncertainty and shrinks the correlation between the slope and intercept errors.

This effect can be visualized as follows. The figure below shows a straight-line fit to scattered data points. The fit line itself does not depend on where the abscissa zero point is, it will always minimize chi-square in the same way no matter where the intercept is defined. Errors in the line solution generally take the form of a rocking up or down at the extremes while passing through the middle of the scatter at more or less the same place. As a result, if the slope is too large, the intercept at x=0 is too small, hence the negative correlation.

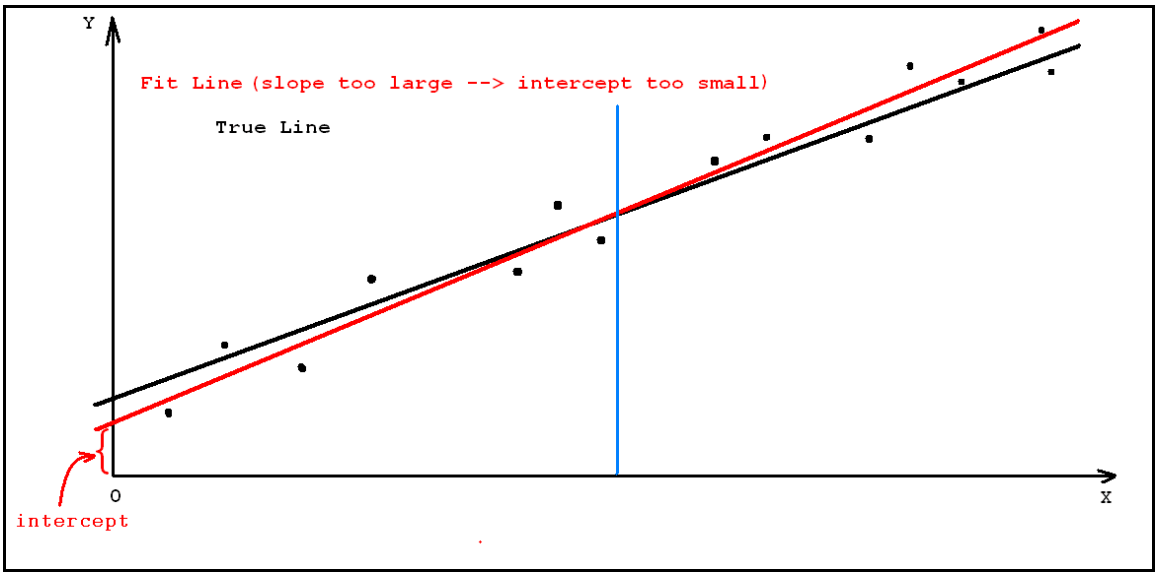

With the zero point defined at x=0, the error covariance matrix will correctly reflect the larger possibility of error in the intercept, and the covariance for the slope and intercept errors will be significantly negative. By the same token, if the intercept is defined to be at a zero point above the abscissa range, the covariance will be positive, as implied in the figure.

If instead a new zero point x_0 is defined, for example at the blue vertical line in the diagram, then the fitting can be done with x-x_0 as the independent variable. The error covariance matrix will then come out with a smaller intercept uncertainty and a significantly reduced off-diagonal covariance for the slope and intercept errors. It must be stressed, however, that whether the zero point is redefined has no effect on the fit or the slope uncertainty, nor is there any effect on the determinant of the error covariance matrix or the uncertainty in points computed from the model.

In our case, the intercept uncertainty is the position uncertainty at the standard epoch, which would be at month m=0 if we do not redefine the zero point. We do in fact redefine it, however, in order to get a truer feel for how accurately the positions can be estimated at the standard epoch, which is now m_0 computed according to

$$\begin{aligned} \sigma^2 &= \left(\sum_{i=1}^{N} \frac{1}{\sigma_{\lambda i}^2} \right)^{-1} \\ m_0 &= \sigma^2 \sum_{i=1}^{N} \frac{m_i}{\sigma_{\lambda i}^2} \end{aligned} \tag{13}$$

i.e., m_0 is the inverse-λ-variance-weighted average of the m_i values. For convenience, and to have the same standard epoch for both λ and β, this was used for both solutions (or both axes could have been used in the summation, but the difference would have been negligible in this simulation). It is not obvious without going through some algebra, but for a pure straight-line fit, this definition minimizes v_{11} in equation 9 and is the solution to the equation v_{12}=0 (see Appendix B). For our three-parameter model, it is not exact, but in practice it appears to be close enough for our purposes. Note that m as used to model the Earth's ecliptic longitude does *not* use this zero-point translation, since the relevant aspect there is the Earth's longitude, not the measurement time explicitly. So the basis functions are

$$\begin{aligned} &f_1 = 1\,,\ f_2 = m - m_0\,,\ f_3 = \sin\left(\lambda - \left(30^\circ (m-2) + 180^\circ\right)\right) \ \text{ for } \lambda \\ &f_1 = 1\,,\ f_2 = m - m_0\,,\ f_3 = \cos\left(\lambda - \left(30^\circ (m-2) + 180^\circ\right)\right)\sin\beta \ \text{ for } \beta \end{aligned} \tag{14}$$

The corresponding model equations are therefore

$$\begin{aligned} \lambda &= \lambda_0 + \mu'_\lambda (m - m_0) + p' \sin(\lambda_0 - \lambda_E) \\ \beta &= \beta_0 + \mu_\beta (m - m_0) + p \cos(\lambda_0 - \lambda_E) \sin\beta \end{aligned} \tag{15}$$

and Equation 6 becomes

$$
\begin{aligned}
b_k &\equiv \sum_{i=1}^{N} \frac{\lambda_i \, f_k(m_i)}{\sigma_i^2} \,, \; k = 1 \text{ to } 3 \\
a_{jk} &\equiv \sum_{i=1}^{N} \frac{f_j(m_i) \, f_k(m_i)}{\sigma_i^2} \,, \; j = 1 \text{ to } 3 \,, \; k = 1 \text{ to } 3
\end{aligned}
\tag{16}
$$

for λ, and similar summations apply for β. The fitting coefficients are then obtained according to Equation 8, and the uncertainty of any value computed from the model equations can be evaluated according to Equation 11. When evaluating the λ model equation, the μ_λ' and p' values should be used, but for quoting the proper motion and parallax in true angular measure for the λ solution, the unprimed values should be used:

$$
\begin{aligned}
\mu_\lambda &= \mu_\lambda' \cos\beta \\
p(\lambda) &= p' \cos\beta
\end{aligned}
\tag{17}
$$

where "$p(\lambda)$" means "p from the λ solution"; there is only one parallax parameter, it just happens to appear in the two separate solutions in this simulation. In the WPHotpm algorithm, a single parallax value will result from the chi-square minimization. For the simulation, a final p estimate is computed via inverse-variance averaging of the values from the two solutions:

$$
\begin{aligned}
\sigma_p^2 &= \left(\frac{1}{\sigma_{p(\lambda)}^2} + \frac{1}{\sigma_{p(\beta)}^2} \right)^{-1} \\
p &= \sigma_p^2 \left(\frac{p(\lambda)}{\sigma_{p(\lambda)}^2} + \frac{p(\beta)}{\sigma_{p(\beta)}^2} \right)
\end{aligned}
\tag{18}
$$

where the variances are obtained from Equation 9 corresponding to the λ and β solutions separately, and the result of that for $\sigma^2_{p(\lambda)}$ has been multiplied by $\cos^2\beta$. In practice, the inefficient β sampling of parallax always produced such a large uncertainty that β contributed essentially nothing to the final estimate.

4. Results

The simulation was run for the baseline strategy described in section 2 for stars at ecliptic latitudes of 0°, 30°, 60°, and 85°, all at ecliptic longitude 90°, and with proper motions of 1 arcsec/yr on each axis, and parallax of 1 arcsec. The measurement uncertainties which served as the 1-sigma values for Gaussian pseudorandom errors ranged from 0.4 to 0.55 arcsec on each axis. The simulated longitude measurements for the 30°-latitude case were shown in a figure in section 2; here we repeat that figure with the solution plotted in blue and the $\pm 3\sigma$ contours shown in red. The scale of the image can be visualized from the fact that the peak-to-peak parallax variations are 2 arcsec full width on average.

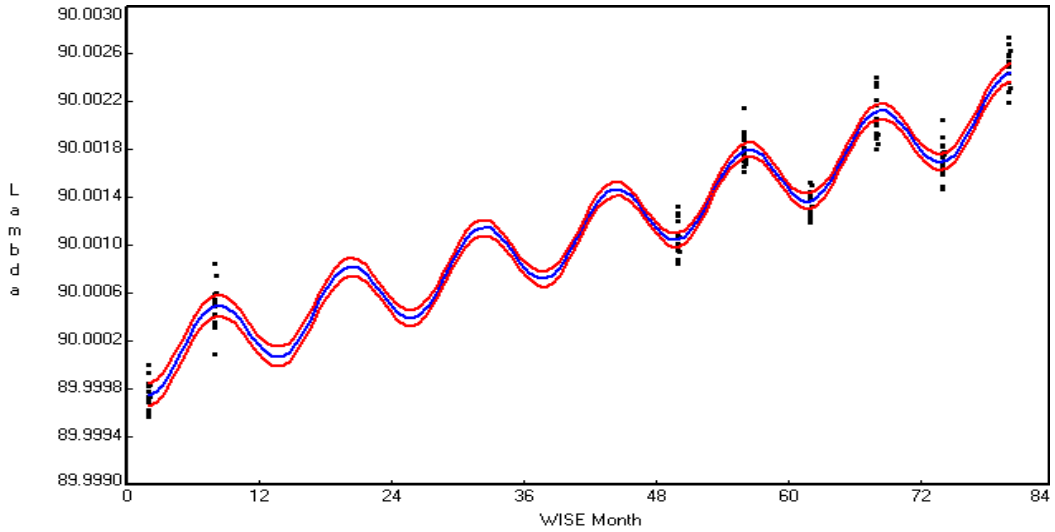

(90,30) test data - Black: Lambda Measurements - Blue: fit - Red: 3-sigma contours

For this case, m_0 took the value 50.592; this is shown as the blue vertical line in the plot below, which shows the one-sigma uncertainty of the longitude model fit.

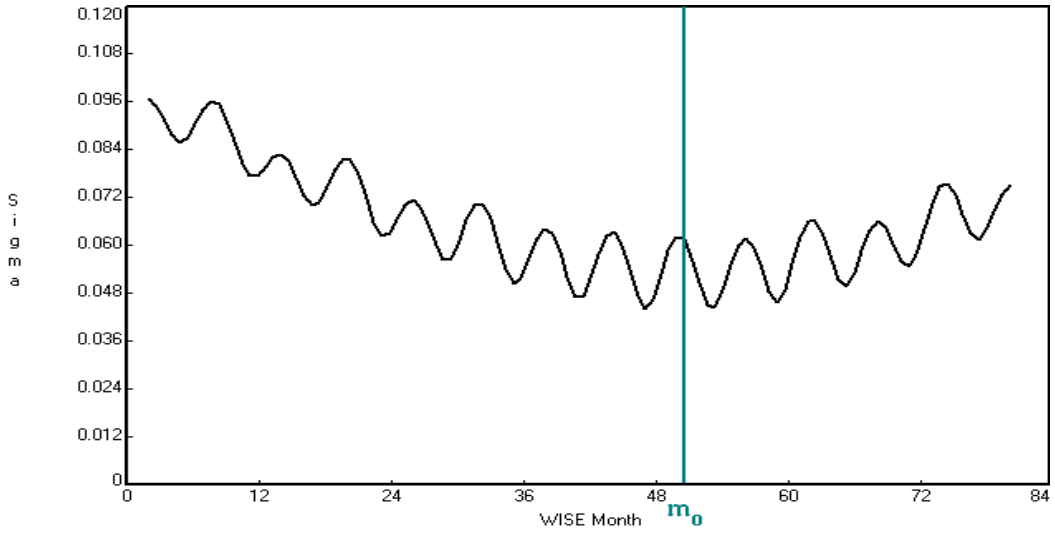

(90,30) test data - Lambda Uncertainty 1-Sigma (arcsec)

The model uncertainty has twice the frequency of the parallax variations. It has local maxima at the parallax extrema and minima at the midpoints between extrema, where the parallax itself is zero. The maxima corresponding to positive parallax extrema are slightly larger than those corresponding to negative parallax extrema. On average, the uncertainty increases away from m_0 because of the uncertainty associated with the proper motion. Since WPHotpm computes motion for an optimal standard epoch, the smaller position uncertainty at the standard epoch is indicative of what to expect from MaxWISE.

A summary of results for the baseline strategy applied to the four latitude cases is as follows, where angle sigma values are in true-angle arcsec, proper motion sigma values are in true-angle arcsec/yr, and $\rho(\lambda_0,\mu_\lambda')$ is the correlation in the errors between λ_0 and λ proper motion.

β	N	$\sigma_{\lambda 0}$	$\sigma_{\beta 0}$	$\sigma_{\mu\lambda}$	$\sigma_{\mu\beta}$	σ_p	$\rho(\lambda_0,\mu_\lambda')$	χ^2_{reduced}
0°	96	0.04808	0.04777	0.02137	0.02092	0.04830	-1.455e-3	0.81259
30°	120	0.04340	0.04244	0.01900	0.01849	0.04374	1.334e-3	1.04405
60°	216	0.03195	0.03241	0.01402	0.01419	0.03215	6.381e-4	1.06243
85°	248	0.02973	0.02987	0.01300	0.01294	0.02987	-6.909e-4	1.17576

Table 4.1: m in (2,8,50,56,62,68,74,80), source position uncertainties 0.40-0.55 arcsec

These results are for source detections with single-frame position uncertainties between 0.4 and 0.55 arcsec on each axis. For sources such as those used for distortion calibration, which have position uncertainties typically from 0.130 to 0.145 arcsec per axis, the results for the second case are as shown below.

β	N	$\sigma_{\lambda 0}$	$\sigma_{\beta 0}$	$\sigma_{\mu\lambda}$	$\sigma_{\mu\beta}$	σ_p	$\rho(\lambda_0,\mu_\lambda')$	χ^2_{reduced}
30°	120	0.01252	0.01256	0.00549	0.00551	0.01259	1.591e-4	1.27664

Table 4.2: m in (2,8,50,56,62,68,74,80), source position uncertainties 0.130-0.145 arcsec

It is seen that the output uncertainties scale approximately with the input uncertainties, and that the parallax uncertainty is very similar to each model standard-epoch position uncertainty. A distortion-calibration source at 30° latitude and a distance of 15.9 parsecs would have its parallax measured with a S/N of 5. The same uncertainty scaling implies that such sources at 60° and 85° would have their parallaxes measured with S/N =5 at distances of 21.5 and 23.1 parsecs, respectively.

These results all use the "baseline" strategy, to which there is no option within 65° of the ecliptic, but we can try some variations for the 85° case. The table on page 1 shows that with two "epochs", AllWISE obtained 128 measurements, or 64 per epoch. Assuming that the same number of measurements per epoch applies to MaxWISE, then we cannot go above 64 measurements on any of the eight epochs, which means that the most extreme endpoint-clustering option is to use the first two and last two epochs, i.e., the orbits centered on m = 2, 8, 74, and 80, with 62 measurements per epoch to keep the total under 250 (we could squeeze in two more by using 63 measurements for the epochs at m = 2

and 80, but for simplicity, the four epochs were kept equal with 62). This case was simulated, and the results were as follows.

β	N	$\sigma_{\lambda 0}$	$\sigma_{\beta 0}$	$\sigma_{\mu\lambda}$	$\sigma_{\mu\beta}$	σ_p	$\rho(\lambda_0,\mu_\lambda')$	χ^2_{reduced}
85°	248	0.02990	0.03005	0.00997	0.00999	0.02999	1.191e-3	1.02221

Table 4.3: m in (2,8,74,80), source position uncertainties 0.40-0.55 arcsec

Comparing these results to those for the baseline strategy (Table 4.1, $\beta =$ 85°), the only significant changes are in the proper motion uncertainties, which drop to about 77% of their previous values. The parallax uncertainty is not impacted because the periodicity is well sampled by having the earlier pair and the later pair of epochs spaced at the minimum possible six months. If this is not done, e.g., if we use epochs with central *m* values in (2,56,62,80), in which only the central pair has the minimum six-month separation, we lose some accuracy in both parallax and proper motion.

β	N	$\sigma_{\lambda 0}$	$\sigma_{\beta 0}$	$\sigma_{\mu\lambda}$	$\sigma_{\mu\beta}$	σ_p	$\rho(\lambda_0,\mu_\lambda')$	χ^2_{reduced}
85°	248	0.02987	0.03100	0.01570	0.01289	0.03800	5.698e-4	0.96832

Table 4.4: m in (2,56,62,80), source position uncertainties 0.40-0.55 arcsec

The model uncertainties for these three $\beta =$ 85° cases are shown below.

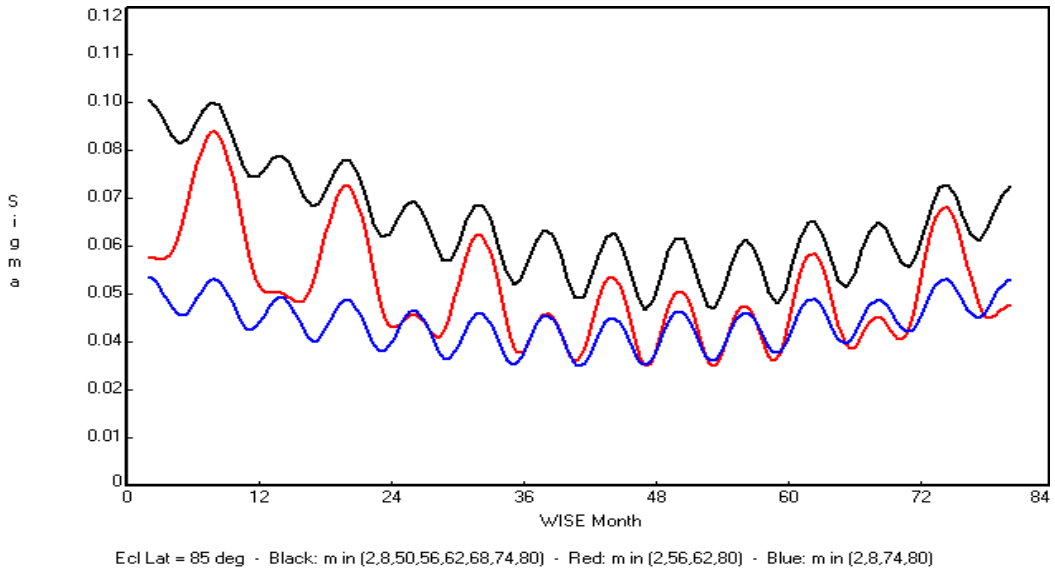

Although it is not possible to use fewer than four epochs and still have a total number of measurements close to 250, it would not be desirable to do so anyway, because tests using 124 measurements each in epochs *m* in (2,80) and (2,74) show that proper motion and parallax cannot be disentangled; the periodicity of parallax must be sampled better than that. Adding one more epoch and using 83 measurements in each of the three helps as long as the additional epoch is only six months from one of the other two, but accuracy is still lost compared to the three cases shown above. For example, with 83

measurements each and m in (2,8,80), the parallax uncertainty increased to 0.03753 arcsec, whereas with m in (2,50,80) it was 0.05201 arcsec, and in both cases proper motion uncertainty increased significantly.

It appears that for both proper motion and parallax, the best attenuation strategy at sufficiently extreme ecliptic latitudes is to use m in (2,8,74,80) with 62 measurements per epoch. This would also provide the best available information on variability at time scales between hours, days, and months, although that loses information on scales of 1-2 years. At less extreme latititudes where fewer than 64 measurements per epoch are available, it appears that the two extreme epoch pairs could be used fully, then one would have to work inward from the late end as possible while keeping each measurement paired with another six months apart in time in order to keep parallax periodicity optimally sampled.

5. Recommendations for MaxWISE Data Products

The results for ecliptic latitude 30^o may be considered typical of what MaxWISE will be able to do. These are a little better than closer to the ecliptic and not as good as closer to the poles, but closer to the poles means occupying a smaller fraction of the sky. At $\beta = 30^o$, proper motion uncertainties range between about 0.0187 arcsec/yr and 0.0055 arcsec/yr for MaxWISE sources of the two quality levels considered, i.e., with single-frame position uncertainties around 0.50 arcsec and 0.15 arcsec per axis, respectively.

The better quality sources are those used for distortion calibration, so we will assume that it would be meaningful to compare those to the UCAC4 sources used for astrometric calibration. Statistics for the UCAC4 sources used for the tile 0908p651 show that the UCAC4 proper-motion uncertainties have a mean of 0.0026 arcsec/yr and a standard deviation of 0.0015 arcsec/yr on each axis. So the mean UCAC4 uncertainties are about half the size of what can be expected from MaxWISE at medium ecliptic latitudes. For MaxWISE to come so close to the gold-standard proper motion catalog argues that MaxWISE will yield a very useful proper motion and parallax catalog for infrared sources.

For this reason it is important that the MaxWISE catalog include all the parameters needed for optimal use of its information, and this will require adding some columns to the multi-frame source-extraction list. Besides the obvious parallax and its uncertainty, these include parameters needed to apply the proper motion and parallax information to times other than the standard epoch.

In order to simplify such a computation, the positions reported as “standard epoch” positions should be those computed for the processing epoch specific to each source, i.e., what is called “m_0” above. This is significantly different for each source, as it was in AllWISE, but in AllWISE, each source’s position was propagated to a single “standard epoch” for the whole catalog, namely JD 2455400.0. Doing this incurred some additional uncertainty which in principle could have been removed if anyone had wished to propagate the positions to a significantly different epoch, but the odds of anyone doing this are extremely small because of the neglecting of parallax and the generally low sensitivity to motion. In AllWISE, the motion solution is primarily just a flag for sources that are probably worthwhile following up with additional observations, not a mechanism for propagating positions in time.

In MaxWISE, with vastly greater sensitivity to motion, both proper motion and parallax, it should be expected that some need to propagate positions to other epochs will arise, and so the products should include all available information for making this computation optimal. Since users will have to read a number of columns from the catalog anyway, it seems that no significant extra burden is levied by including the source-specific epoch among such columns, and this removes the need to propagate to a catalog-specific standard epoch with the extra error induced by that quite unnecessarily. So this change for MaxWISE would be a change in meaning of the existing AllWISE columns, i.e., RA and Dec and their uncertainties would refer to the source-specific epoch, not a one-epoch-for-all.

The other changes needed are the inclusion of the three off-diagonal elements of the error covariance matrix for each axis. Although using the MaxWISE equivalent of m_0 as the standard epoch reduces the magnitudes of these off-diagonal elements, the process is inexact because of the presence of parallax in the model, and neglecting them in the uncertainty propagation could be a serious error for propagations over relatively long time intervals. The source list should therefore include columns for all six parameters needed to evaluate the last line of Equation 11 for each axis.

Evaluating the MaxWISE model to propagate position would therefore be similar to how it is done in this simulation, e.g., for RA

$$\begin{aligned}
\alpha &= \alpha_0 + \mu'_\alpha\,(t - t_0) + p'\,g(\alpha_0, \delta_0, \vec{v}_E) \\
\sigma^2_\alpha &= \sigma^2_{\alpha 0} + \sigma^2_{\mu'\alpha}(t - t_0)^2 + \sigma^2_{p'}\,g^2(\alpha_0, \delta_0, \vec{v}_E) \\
&\quad + 2\,\mathrm{cov}(\alpha_0, \mu'_\alpha)(t - t_0) + 2\,\mathrm{cov}(\alpha_0, p')g(\alpha_0, \delta_0, \vec{v}_E) \\
&\quad + 2\,\mathrm{cov}(\mu'_\alpha, p')(t - t_0)g(\alpha_0, \delta_0, \vec{v}_E)
\end{aligned} \tag{19}$$

where the primes indicate quantities in azimuthal RA angle, and the *g* function expresses the projection of unit parallax onto the RA axis, analogous to the *g* functions for ecliptic coordinates in Equation 12.

The WPHotpm chi-square minimization algorithm solves for fluxes and positions at the same time. This requires a nonlinear technique that takes the form of a numerical search in parameter space for the minimum value of chi-square. Such techniques are typically sensitive to the initial parameter estimates, because noise can cause many local minima to exist. For the AllWISE motion solution, the best results for known moving objects were found by using a standard epoch (what corresponds to m_0 herein) computed as the flux-weighted mean observation epoch. Several other methods were also implemented and tested, some of which worked as well, but since none were noticeably better than the flux-weighted mean, that was kept in the processing. Given the algebraic justification for the use of inverse-variance weighting (see Appendix B), it is recommended to switch the default for MaxWISE to that method, which amounts to using "MeanObsEpochType = 4" in the namelist input.

Appendix A: The MaxWISE First Data Release

The methods discussed above can be applied to the time period whose data will constitute the MaxWISE First Data Release. This time period, expressed in "WISE Months" extends from $m = 0$ to $m = 60$, of course with the gap from $m = 12$ to $m = 48$. The simulated case for 30° ecliptic latitude with m in the set (2,8,50,56,62,68,74,60) can be analyzed for the reduced set (2,8,50,56) to determine the extent to which information is lost compared to MaxWISE but gained relative to AllWISE. Already a known moving object has been processed for three epochs and found to have a greatly reduced motion uncertainty.

The MaxWISE First Data Release will not have included parallax in the analysis, but we can look at the simulated data with and without parallax. Since most objects will have negligible parallax, the position and slope uncertainties of a straight-line fit to the positions will be a good indication of what can be expected to be meaningful. Of course, since these uncertainties are independent of the actual motion and parallax, when parallax is significant, the fit chi-square will inflate, but the uncertainties will remain the same. We saw above that any three WISE epochs, as long as two have a six- month separation, can sense parallax rather well, so even in AllWISE there are a few sources that could be fit to the full MaxWISE model.

The case with ecliptic coordinates (90°,30°) and position uncertainties in the range 0.40 to 0.55 arcsec was run for the m sets (2,8,50,56) and (2,8,50) using the full MaxWISE model and also using a straight-line fit. Recall that these m values are approximate, i.e., the "2" really represents a set of multiple measurements taken one orbit apart centered on $m = 2$. Since at 30° latitude there are 15 measurements for each of these observation opportunities, the two sets comprise 60 and 45 measurements respectively, and that is how these cases are distinguished in Table A.1 below, where the results are given along with the full MaxWISE case.

β	N	$\sigma_{\lambda 0}$	$\sigma_{\beta 0}$	$\sigma_{\mu\lambda}$	$\sigma_{\mu\beta}$	σ_p	$\rho(\lambda_0,\mu_\lambda')$	χ^2_{reduced}
30°	120	0.04340	0.04244	0.01900	0.01849	0.04374	1.334e-3	1.04405
30°	60	0.06176	0.06016	0.03089	0.03000	0.06207	2.154e-3	0.84698
30°	45	0.07502	0.11105	0.04415	0.09240	0.08163	0.132266	0.91607

Table A.1: Source position uncertainties 0.40-0.55 arcsec

Normally the position uncertainties are about the same for longitude and latitude, but as the sampling becomes insufficient to support parallax estimation, the presence of parallax in the model causes errors and uncertainties to bleed into the other terms, especially for latitude, where the parallax sampling is never good. This is seen in the three-epoch case, where the latitude position uncertainty becomes noticeably larger than the longitude uncertainty.

These cases were also run through a straight-line fitting algorithm for longitude with the following results. The absence of a partially confounding parallax term allows the straight line fit uncertainties to be quite a bit smaller, but since this case also had the same proper motion and parallax as before, namely 1 arcsec/yr proper motion and 1 arcsec of parallax, the small uncertainties can be seen to be

unrealistic by the size of the reduced chi-squares. In most cases, with very small parallax, these chi-squares would be much better, and the small uncertainties would actually be of value. Since only longitude was fit, the latitude columns in the previous table are used below to copy the MaxWISE longitude values for comparison to the straight-line fit. We also add a line at the bottom for the AllWISE linear fit; there is no corresponding MaxWISE model because of the total coupling between parallax and the other two parameters.

β	N	$\sigma_{\lambda 0}$	$A.1\ \sigma_{\lambda 0}$	$\sigma_{\mu\lambda}$	$A.1\ \sigma_{\mu\lambda}$	σ_p	$\rho(\lambda_0,\mu_\lambda')$	χ^2_{reduced}
30°	120	0.03759	0.04340	0.01633	0.01900	N/A	3.150e-16	6.79328
30°	60	0.05348	0.06176	0.02662	0.03089	N/A	4.818e-16	7.47938
30°	45	0.06154	0.07502	0.03484	0.04415	N/A	2.920e-16	6.25881
30°	30	0.07505	N/A	0.30052	N/A	N/A	1.073e-16	1.39339

Table A.2: Straight-line longitude fits, source position uncertainties 0.40-0.55 arcsec

The straight-line fit to longitude for the entire MaxWISE period is shown in red below with the MaxWISE fit in black.

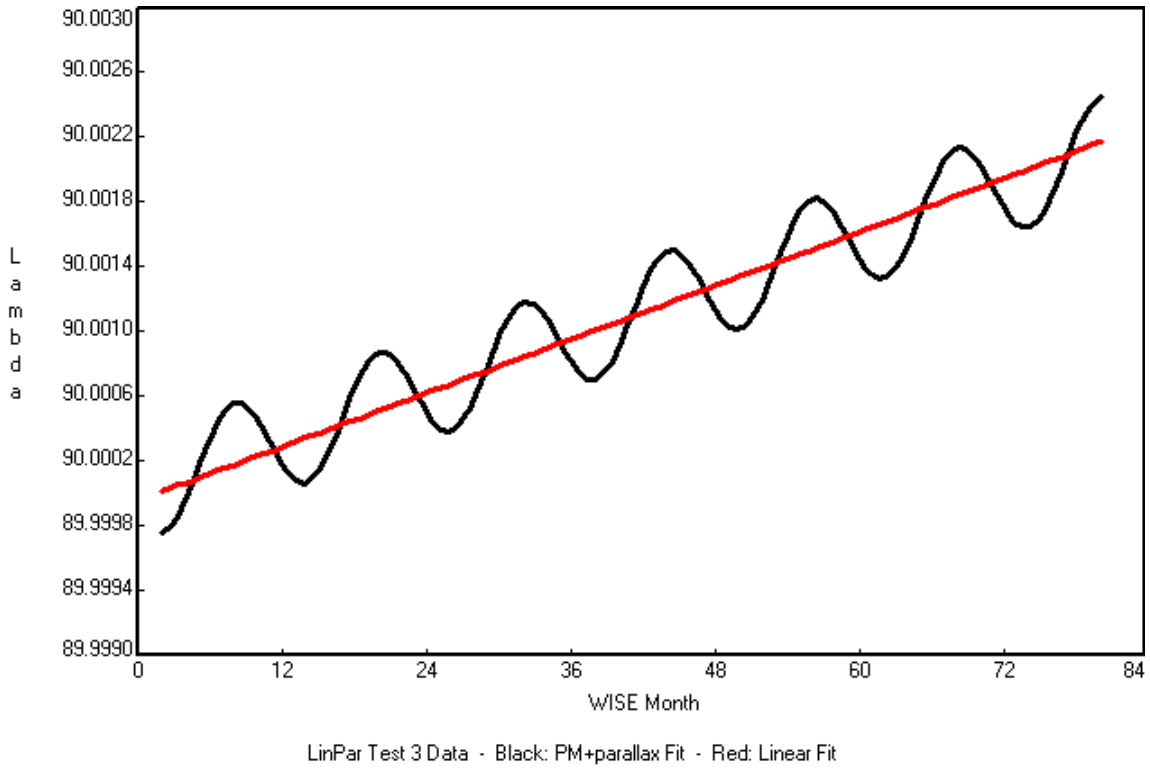

The small slope and intercept uncertainties certify that of all possible straight-line fits to the data, the one obtained is very close to being the best; whether the fit is actually any good can be revealed only by the chi-square figure of merit. If the parallax amplitude had been very small, then the straight-line

would actually be preferable, because its lack of a parallax term precludes the extra uncertainty.

The longitude model uncertainties for these six cases are shown for the First Release period below. The oscillatory curves are for the full MaxWISE model.

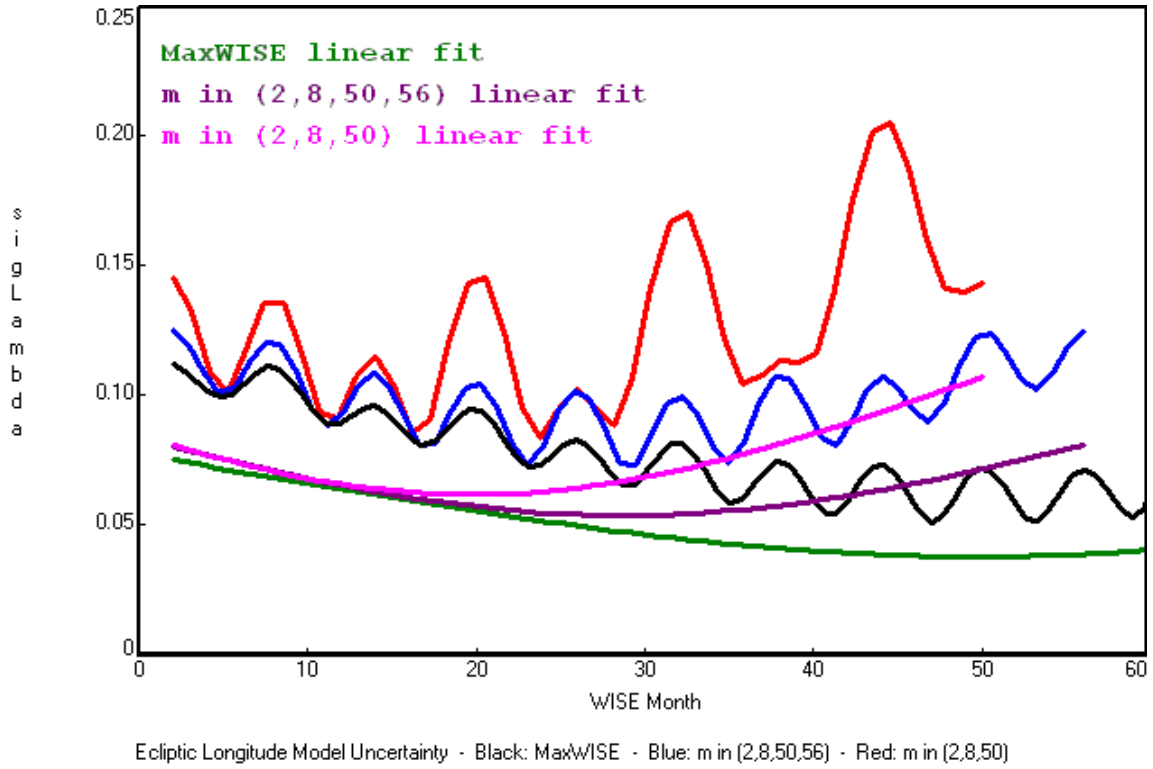

Ecliptic Longitude Model Uncertainty - Black: MaxWISE - Blue: m in (2,8,50,56) - Red: m in (2,8,50)

The red curve shows how the parallax uncertainty is quite large with only three “epochs” (45 measurements and minimal parallax sampling), and yet it is not unusable, especially considering that the source simulated had the larger of the two classes of position uncertainty. The other class, corresponding to sources used for distortion calibration, would have similar shapes but a different ordinate scale, reduced by about a factor of three.

Appendix B: The Optimum Zero Point

For a straight-line model in a chi-square minimization, the basis functions are

$$\begin{aligned} f_1(x) &= (x - x_0)^0 = 1 \\ f_2(x) &= (x - x_0)^1 = (x - x_0) \end{aligned} \tag{B.1}$$

where we include the abscissa zero point x_0 explicitly. Then Equation 6 becomes

$$\begin{aligned} a_{11} &= \sum_{i=1}^{N} \frac{1}{\sigma_i^2} \\ a_{12} &= a_{21} = \sum_{i=1}^{N} \frac{(x_i - x_0)}{\sigma_i^2} \\ a_{22} &= \sum_{i=1}^{N} \frac{(x_i - x_0)^2}{\sigma_i^2} \end{aligned} \tag{B.2}$$

The coefficient matrix and its determinant are

$$\begin{aligned} A &= \begin{pmatrix} a_{11} & a_{12} \\ a_{12} & a_{22} \end{pmatrix} \\ D &= a_{11} a_{22} - a_{12}^2 \end{aligned} \tag{B.3}$$

where we used $a_{12} = a_{21}$ explicitly. The error covariance matrix Ω is the inverse of A:

$$\Omega = A^{-1} = \begin{pmatrix} \frac{a_{22}}{D} & \frac{-a_{12}}{D} \\ \frac{-a_{12}}{D} & \frac{a_{11}}{D} \end{pmatrix} \equiv \begin{pmatrix} v_{11} & v_{12} \\ v_{12} & v_{22} \end{pmatrix} \tag{B.4}$$

The optimum value for x_0 is that which minimizes v_{11} and makes v_{12} zero. We may assume that $D \neq 0$ because if $D = 0$ the system of equations we want to solve in the chi-square minimization would be singular. We also know that $D > 0$, because the determinant of the error covariance matrix is $1/D$ and is proportional to the area of the error ellipse. which must be positive for physically real applications. Furthermore, the determinant D does not depend on x_0 at all, since the latter cancels out of the former:

$$
\begin{aligned}
D &= \left(\sum_{i=1}^{N}\frac{1}{\sigma_i^2}\right)\left(\sum_{i=1}^{N}\frac{(x_i-x_0)^2}{\sigma_i^2}\right)-\left(\sum_{i=1}^{N}\frac{(x_i-x_0)}{\sigma_i^2}\right)^2 \\
&= \left(\sum_{i=1}^{N}\frac{1}{\sigma_i^2}\right)\left(\sum_{i=1}^{N}\frac{x_i^2}{\sigma_i^2}-2\sum_{i=1}^{N}\frac{x_i x_0}{\sigma_i^2}+\sum_{i=1}^{N}\frac{x_0^2}{\sigma_i^2}\right)-\left(\sum_{i=1}^{N}\frac{x_i}{\sigma_i^2}-\sum_{i=1}^{N}\frac{x_0}{\sigma_i^2}\right)^2 \\
&= \left(\sum_{i=1}^{N}\frac{1}{\sigma_i^2}\right)\left(\sum_{i=1}^{N}\frac{x_i^2}{\sigma_i^2}-2x_0\sum_{i=1}^{N}\frac{x_i}{\sigma_i^2}+x_0^2\sum_{i=1}^{N}\frac{1}{\sigma_i^2}\right)-\left(\sum_{i=1}^{N}\frac{x_i}{\sigma_i^2}\right)^2+2x_0\left(\sum_{i=1}^{N}\frac{1}{\sigma_i^2}\right)\left(\sum_{i=1}^{N}\frac{x_i}{\sigma_i^2}\right)-x_0^2\left(\sum_{i=1}^{N}\frac{1}{\sigma_i^2}\right)^2 \\
&= \left(\sum_{i=1}^{N}\frac{1}{\sigma_i^2}\right)\left(\sum_{i=1}^{N}\frac{x_i^2}{\sigma_i^2}\right)-\left(\sum_{i=1}^{N}\frac{x_i}{\sigma_i^2}\right)^2 \\
&\quad +2x_0\left(\left(\sum_{i=1}^{N}\frac{1}{\sigma_i^2}\right)\left(\sum_{i=1}^{N}\frac{x_i}{\sigma_i^2}\right)-\left(\sum_{i=1}^{N}\frac{1}{\sigma_i^2}\right)\left(\sum_{i=1}^{N}\frac{x_i}{\sigma_i^2}\right)\right)+x_0^2\left(\left(\sum_{i=1}^{N}\frac{1}{\sigma_i^2}\right)^2-\left(\sum_{i=1}^{N}\frac{1}{\sigma_i^2}\right)^2\right) \\
&= \left(\sum_{i=1}^{N}\frac{1}{\sigma_i^2}\right)\left(\sum_{i=1}^{N}\frac{x_i^2}{\sigma_i^2}\right)-\left(\sum_{i=1}^{N}\frac{x_i}{\sigma_i^2}\right)^2
\end{aligned}
\tag{B.5}
$$

So we need not be concerned with any dependence of D on x_0 when solving for $v_{12} = 0$ and when minimizing v_{11}. In the former case, we have

$$
\begin{aligned}
&\sum_{i=1}^{N}\frac{x_i - x_0}{\sigma_i^2} = 0 = \sum_{i=1}^{N}\frac{x_i}{\sigma_i^2} - \sum_{i=1}^{N}\frac{x_0}{\sigma_i^2} \\
&\sum_{i=1}^{N}\frac{x_i}{\sigma_i^2} = \sum_{i=1}^{N}\frac{x_0}{\sigma_i^2} = x_0\sum_{i=1}^{N}\frac{1}{\sigma_i^2} \\
&x_0 = \frac{\sum_{i=1}^{N}\frac{x_i}{\sigma_i^2}}{\sum_{i=1}^{N}\frac{1}{\sigma_i^2}}
\end{aligned}
\tag{B.6}
$$

This is the same result we get when we minimize v_{11}:

$$
\begin{aligned}
\frac{\partial v_{11}}{\partial x_0} &= \frac{1}{D}\left(\frac{\partial a_{22}}{\partial x_0}\right) = \frac{1}{D}\left(\frac{\partial}{\partial x_0}\sum_{i=1}^{N}\frac{(x_i-x_0)^2}{\sigma_i^2}\right) \\
&= \frac{-2}{D}\sum_{i=1}^{N}\frac{(x_i-x_0)}{\sigma_i^2} = 0 \Rightarrow \sum_{i=1}^{N}\frac{(x_i-x_0)}{\sigma_i^2} = 0
\end{aligned}
\tag{B.7}
$$

which is the same equation we solved above, so it has the same solution as Equation B.6. A quick check of the second derivative shows that it is positive, hence we have a minimum for v_{11}:

$$\frac{\partial^2 v_{11}}{\partial^2 x_0} = \frac{2}{D}\sum_{i=1}^{N}\frac{1}{\sigma_i^2} > 0 \qquad \text{(B.8)}$$

The choice of x_0 does not affect v_{22}, the slope uncertainty, since it is a_{11}/D, and as seen in Equation B.2, a_{11} depends only on the measurement uncertainties.

The situation becomes more complicated when the parallax term is added to the model. The definition of a_{12} in Equation B.2 no longer applies, and the solution for x_0 in Equation B.6 no longer makes v_{12} exactly zero. It can be seen in Table A.2 that the computed correlation is on the order of 10^{-16} for these linear fits; the failure to be exactly zero is due to numerical roundoff error. Tables 4.1 and 4.2 show the correlation for the full MaxWISE model using the computed almost-optimal zero point to be on the order of 10^{-3}. When the zero point is left at zero, however, this correlation is about -0.88 in all cases, so a drop to 10^{-3} is substantial.

A numerical experiment was done for the (90^o,30^o) case to find the value of the zero point that produced zero correlation; this was found to be about 49.59163, which is quite close to the inverse-variance-weighted solution, 49.6281860, for which the correlation was 0.0013336. Given the increased complication required to compute a zero point that would produce formally a zero correlation, a difference of 0.0366 months seems not worth the extra effort, especially as long as the recommendation to use the full error covariance matrix in computing model uncertainties is followed. Furthermore, as will be shown below, the optimal zero point for one axis is generally not the same as that for the other, so there is no one zero point that is perfectly optimal globally. In principle, each axis could be assigned its own zero point, but it is unlikely that such an entanglement would be judged necessary or acceptable.

Even though the model uncertainty is unaffected by the zero point as long as the rigorous formula is used to compute it, it is still important to use an almost-optimal zero point in the real MaxWISE chi-square minimization, because the nonlinear numerical-search algorithm works best when started close to the solution, and we assume that MaxWISE will maintain the AllWISE approach of using the stationary-solution positions as starting estimates for the full model, since these appeared to work well when associated with their optimal zero-point epochs. The real MaxWISE algorithm treats both position axes and all fluxes as part of a single system with a single error covariance matrix, and its input uncertainties apply to flux, not position. Since, as we will see below, the epoch zero point that zeroes out the correlation for longitude is not quite equal to that for latitude, it seems likely that this will also be true for the real MaxWISE algorithm, making the simpler computation that much more desirable.

It is still of interest to illustrate how the error covariance matrix changes when we add the parallax term. We will consider just the longitude equation. Using the basis functions shown in Equation 14 and the simulation notation:

$$f_1 = 1\,,\ f_2 = m - m_0\,,\ f_3 = g(\lambda,m) = \sin\left(\lambda - \left(30^\circ(m-2) + 180^\circ\right)\right) \qquad \text{(B.9)}$$

The elements of the coefficient matrix are

$$
\begin{aligned}
a_{11} &= \sum_{i=1}^{N} \frac{1}{\sigma_i^2} \\
a_{12} &= a_{21} = \sum_{i=1}^{N} \frac{m_i - m_0}{\sigma_i^2} \\
a_{13} &= a_{31} = \sum_{i=1}^{N} \frac{g(\lambda, m_i)}{\sigma_i^2} \\
a_{22} &= \sum_{i=1}^{N} \frac{(m_i - m_0)^2}{\sigma_i^2} \\
a_{23} &= a_{32} = \sum_{i=1}^{N} \frac{(m_i - m_0) g(\lambda, m_i)}{\sigma_i^2} \\
a_{33} &= \sum_{i=1}^{N} \frac{g^2(\lambda, m_i)}{\sigma_i^2}
\end{aligned}
\tag{B.10}
$$

The A matrix and its determinant D are (again writing the symmetry explicitly)

$$
\begin{aligned}
A &= \begin{pmatrix} a_{11} & a_{12} & a_{13} \\ a_{12} & a_{22} & a_{23} \\ a_{13} & a_{23} & a_{33} \end{pmatrix} \\
D &= a_{11} a_{22} a_{33} + 2 a_{12} a_{13} a_{23} - a_{11} a_{23}^2 - a_{12}^2 a_{33} - a_{13}^2 a_{22}
\end{aligned}
\tag{B.11}
$$

As before, the zero point cancels out of the determinant (the proof is omitted for brevity). The error covariance matrix is

$$
\Omega = A^{-1} = \frac{1}{D} \begin{pmatrix} a_{22} a_{33} - a_{23}^2 & -a_{12} a_{33} + a_{13} a_{23} & a_{12} a_{23} - a_{13} a_{22} \\ -a_{12} a_{33} + a_{13} a_{23} & a_{11} a_{33} - a_{13}^2 & a_{11} a_{23} - a_{12} a_{13} \\ a_{12} a_{23} - a_{13} a_{22} & a_{11} a_{23} - a_{12} a_{13} & a_{11} a_{22} - a_{13}^2 \end{pmatrix} \equiv \begin{pmatrix} v_{11} & v_{12} & v_{13} \\ v_{12} & v_{22} & v_{23} \\ v_{13} & v_{23} & v_{33} \end{pmatrix} \tag{B.12}
$$

Since a_{11}, a_{13}, and a_{33} do not depend on m_0 and are computable before doing the chi-square minimization, they can be considered simply constants. The correlation that we wish to force to zero is $\rho_{12} = v_{12}/\sqrt{(v_{11} v_{22})}$. As previously stated, the diagonal elements are always greater than zero for real applications, so ρ_{12} will be zero if and only if v_{12} is zero. Setting v_{12} to zero and abbreviating $g(\lambda, m_i)$ as g_i implies

$$
\begin{aligned}
a_{33}\sum_{i=1}^{N}\frac{m_i - m_0}{\sigma_i^2} &= a_{13}\sum_{i=1}^{N}\frac{(m_i - m_0)g_i}{\sigma_i^2} \\
a_{33}\sum_{i=1}^{N}\frac{m_i}{\sigma_i^2} - a_{33}\sum_{i=1}^{N}\frac{m_0}{\sigma_i^2} &= a_{13}\sum_{i=1}^{N}\frac{m_i g_i}{\sigma_i^2} - a_{13}\sum_{i=1}^{N}\frac{m_0 g_i}{\sigma_i^2} \\
a_{33}\sum_{i=1}^{N}\frac{m_i}{\sigma_i^2} - a_{33}m_0 a_{11} &= a_{13}\sum_{i=1}^{N}\frac{m_i g_i}{\sigma_i^2} - a_{13}^2 m_0 \\
a_{33}\sum_{i=1}^{N}\frac{m_i}{\sigma_i^2} - a_{13}\sum_{i=1}^{N}\frac{m_i g_i}{\sigma_i^2} &= m_0(a_{33}a_{11} - a_{13}^2) \\
m_0 &= \frac{1}{a_{33}a_{11} - a_{13}^2}\left(a_{33}\sum_{i=1}^{N}\frac{m_i}{\sigma_i^2} - a_{13}\sum_{i=1}^{N}\frac{m_i g_i}{\sigma_i^2}\right)
\end{aligned}
\tag{B.13}
$$

When this formula is used for the (90°,30°) case, it yields a value of 49.591631071261496, essentially what was found numerically, 49.59163. The correlation ρ_{12} was zero to all ten displayed decimal places, but the corresponding ρ_{12} for latitude was 0.00301, not much less than with the simple zero point, for which the latitude ρ_{12} was 0.00434. Using the formula in Equation B.13 above applied to latitude produced a zero point of 49.508697642255136, for which the latitude ρ_{12} was then reduced to zero to all ten displayed decimal places, but the longitude ρ_{12} was then -0.00303.

Besides forcing v_{12} to zero, the formula in Equation B.13 also minimizes v_{11}, as can be easily verified by taking the derivative of v_{11} with respect to m_0, setting it to zero, and solving for m_0. The last line of Equation B.13 is once again obtained. The second derivative is also easily shown to be positive, so the solution is a minimum for v_{11}. The difference in position uncertainty between the simple zero point (Equation B.6) and that including parallax (Equation B.13) is quite small. For the (90°,30°) case, the longitude uncertainty for the former is 0.0434024734 arcsec, and for the latter it is 0.0434024348, an improvement of only 3.86×10^{-8} arcsec. Equation B.13 applied to latitude yields a latitude uncertainty of 0.0424427475 arcsec, which is 3.99×10^{-7} arcsec smaller than with the simple zero point computed for longitude and used for both axes. Clearly the simple formula that is already implemented in WPHotpm is sufficient.

Appendix C: The MaxWISE Simulation Utilities

The simulations described above can be run by using two utility programs, one to generate the simulated observations, and one to perform the chi-square minimization. Each program is contained in a single file of Fortran source code residing in /home/jwf/src on the IPAC network, and each executable resides in /home/jwf/bin. The programs are named `mwsim` (produces simulated observations for MaxWISE) and `linpar` (linear-plus-parallax fit).

C.1 Simulation (`mwsim`)

The tutorial display is:

```
>mwsim
 usage: mwsim -i infile -o outfile <options>

 where: infile is the name of a file containing values of m to
        be simulated as MaxWISE position measurements, one m
        value per line, header lines beginning with "\" or "|"
        will be ignored

        outfile is the name of the table file for use with the
        linpar program

        optional specifications are:
        -lam   lambda  source ecliptic longitude at m = 0 (deg)
        -bet   beta    source ecliptic latitude at m = 0 (deg)
        -sig   sigma   minimum position uncertainty (asec)
        -dsig  dsig    uniformly distributed random addition to
                       sigma for each simulated position
                       uncertainty (asec)
        -mulam mulam   longitude proper motion (asec/yr)
        -mubet mubet   latitude proper motion (asec/yr)
        -par   par     parallax (asec)
        -nm    nm      no. of m values to generate centered on
                       each input m value and separated by one
                       orbital period
        -rand  rand0   initial random number seed; negative value
                       randomizes, positive repeats sequence

        default values are:
        -lam   90.0
        -bet   30.0
        -sig   0.25
        -dsig   0.1
        -mulam  1.0
        -mubet -1.0
        -par    1.0
        -nm       1
        -rand    -1
```

The input file is a text file containing one number per line representing a “WISE month” as defined above. These can be a complete list of all *m* values for which simulated longitude and latitude position measurements are desired, or they can be just a single *m* value for each “observation epoch”, i.e., a

period of time in which the target is observed on multiple successive orbits. For the latter, the command-line parameter "`-nm`" must be specified. The program does not enforce WISE observing constraints, so it is up to the user to make the geometry realistic, i.e., to specify *m* values for which the specified longitude ("`-lam`") is observable with a solar elongation of about 90°. Since the simulated true longitude has no effect, it is easiest just to keep it at 90° and use "observation epochs" in the set (2,8,50,56,62,68,74,80), since these correspond to times when the WISE spacecraft's ecliptic longitude corresponds to an equinox, hence 90° away from the target star.

The simulated position uncertainties will be uniformly distributed between `sigma` ("`-sig`") and `sigma+dsig` (the latter specified via "`-dsig`"). The independent measurement errors will be drawn from a zero-mean Gaussian population with a standard deviation given by the corresponding uncertainty (hence the reduced chi-square computed by the fitting program should always be fairly close to 1.0). A given pseudorandom sequence may be repeated by making all the corresponding runs with the same positive integer value of `rand0` ("`-rand`"); negative values will cause internal randomization (not repeated sequences), but since this is the default, it need not be specified.

As an example, the run which produced the data for the (2,8,50,56) first-release case was:

```
>mwsim -i x:q -o lptest11.tbl -nm 15 -mubet 1 -sig 0.4 -dsig 0.15
```

where the input file contained the text:

```
2
8
50
56
```

The output file is a table file with the columns

```
1: m
2: Lambda
3: SigLambda
4: Beta
5: SigBeta
6: ParLam
7: ParBeta
```

The chi-square minimzation program `linpar` reads the first five columns in order (it does not use the table header information, which is there only so that plots may be made). The last two columns are for perusing by the user only; they are ignored by `linpar`; they give the parallax projected onto the axes indicated.

C.2 Chi-square Minimization (`linpar`)

The tutorial display is:

```
>linpar
 usage: linpar filename <m0 <out.tbl>>
 where: filename is the name of a file containing values of m,
        lambda, siglambda, beta, and sigbeta to be used in a chi-
        square minimization fit; each line must contain one set
        of (m,lambda,siglambda,beta,sigbeta) values separated by
        blanks in that order; table headers will be skipped

 m is the month of observation by WISE (0-84); at m = 2,
 the sun-to-WISE vector points to the autumnal equinox; lambda is
 the ecliptic longitude observed for the star, and siglambda is
 the uncertainty of lambda (true angle); beta is the ecliptic
 latitude, and sigbeta is the uncertainty of beta

 m0 is an optional fitting zero point for the m data; if
 specified, it will be subtracted from all m values; i.e.,
 m0 is the standard epoch for the position solution, it does
 not change the relation between m and the sun-to-WISE vector;
 specifying m0 as "c" instead of a number will cause m0 to be
 computed to minimize the error correlation between position
 and proper motion

 out.tbl is an optional output table file containing
 the model evaluated at uniformly spaced m values over
 the input range and also the model uncertainty sigma
 and columns containing the model plus/minus sigma and
 plus/minus 3 sigma
```

As an example, the run for the full MaxWISE (90^o,30^o) case with computed m_0 and its stdout was:

```
>linpar lptest3c.tbl c lpt3c-c.tbl
 m0: 49.628185988403295

 No. points: 120
 Full-model lambda computed m0: 49.591631071261496
 Full-model beta computed m0: 49.508697642255136

 lam = f(m) = 90.00132175071765 + 0.000026213188901470954 * ( m -49.628185988403295 )
            + 0.00032139150501571536 * sin(lam-Earthlam)

                     lam(m0): 90.00132175071765 deg
         lam(m0) uncertainty: 0.043402473415750625 arcsec
                   mu(lamda): 0.9809890890513622 arcsec/yr
       mu(lamda) uncertainty: 0.019000425129778956 arcsec/yr
             lambda parallax: 1.0022993924905517 arcsec
 lambda parallax uncertainty: 0.0437412794000477 arcsec

 error covariance matrix determinant: 9.674981518842688E-33

    correlation coefficients:
    1.0000000000   0.0013335626  -0.0108371671
    0.0013335626   1.0000000000  -0.1218497220
   -0.0108371671  -0.1218497220   1.0000000000
```

```
beta = g(m) = 30.00116193659057 + 0.00002371587708823304 * ( m - 49.628185988403295 )
            + 0.0023220982880216706 * cos(lam-Earthlam)*sin(beta)

                   beta(m0): 30.00116193659057 deg
       beta(m0) uncertainty: 0.042443146717608335 arcsec
                   mu(beta): 1.0245258902116672 arcsec/yr
       mu(beta) uncertainty: 0.018487240739274366 arcsec
              beta parallax: 8.359553836878014 arcsec
  beta parallax uncertainty: 3.5026392658001906 arcsec

error covariance matrix determinant: 2.3718952321808596E-29

   correlation coefficients:
   1.0000000000   0.0043371938   0.0812708646
   0.0043371938   1.0000000000   0.0956777488
   0.0812708646   0.0956777488   1.0000000000

          combined parallax: 1.003446595272429 arcsec
 comb. parallax uncertainty: 0.04373786901958137 arcsec

  lam reduced chi-square: 0.6538672670125354
       lam Q(chi-square): 0.9986041446467089

 beta reduced chi-square: 0.9713036341307548
      beta Q(chi-square): 0.5706057199416368

total reduced chi-square: 0.8125854505716451
     total Q(chi-square): 0.9837602025359504
```

The optional output file is a table file useful for plotting purposes and containing the columns:

```
   1: m
   2: Lambda
   3: SigLambda
   4: SigLamTrue
   5: LampSig
   6: LammSig
   7: Lamp3sig
   8: Lamm3sig
   9: LamSig11
  10: LamSig22
  11: LamSig33
  12: LamSig12
  13: LamSig13
  14: LamSig23
```

Column 3 is the uncertainty in the azimuthal angle `Lambda`, while column 4 is this uncertainty expressed in true angular measure. Columns 5 and 6 are `Lambda±SigLambda`, and columns 7 and 8 are `Lambda±3*SigLambda` (for better visibility in a plot). The last six columns are the individual independent components of the error covariance matrix expressed in the sigma domain (with the usual sign conventions).